NASA TECHNICAL NOTE

NASA TN D-5069

c. 1

NASA TN D-5069

IDENTIFICATION OF STRUCTURAL SYSTEMS BY USE OF NEAR-RESONANCE TESTING

by John P. Raney and James T. Howlett

Langley Research Center
Langley Station, Hampton, Va.

NATIONAL AERONAUTICS AND SPACE ADMINISTRATION • WASHINGTON, D. C. • FEBRUARY 1969

NASA TN D-5069

IDENTIFICATION OF STRUCTURAL SYSTEMS BY USE OF NEAR-RESONANCE TESTING

By John P. Raney and James T. Howlett

Langley Research Center
Langley Station, Hampton, Va.

NATIONAL AERONAUTICS AND SPACE ADMINISTRATION

For sale by the Clearinghouse for Federal Scientific and Technical Information
Springfield, Virginia 22151 – CFSTI price $3.00

IDENTIFICATION OF STRUCTURAL SYSTEMS BY USE OF NEAR-RESONANCE TESTING*

By John P. Raney and James T. Howlett
Langley Research Center

SUMMARY

A recent innovation for determining the governing differential equations of motion of a complex structure is described. Numerical values for the mass, stiffness, and damping coefficients of the dynamical equations associated with a particular input response or transmission path are computed from the data usually obtained in conventional vibration tests of a structure. The theory is based on the dynamic properties of multidegree-of-freedom linear systems. The method requires the steady-state response (acceleration, velocity, or displacement) and the driving sinusoidal force input for transmission paths of interest to be determined experimentally for a few frequencies near each major structural resonance. Application of the method is illustrated by determining from experimental data the equations of motion of the 1/10-scale and 1/40-scale models of the Apollo-Saturn V launch vehicle with cantilevered-free and free-free boundary conditions, respectively. Transient responses computed by using the identified equations for the 1/40-scale model are shown to agree favorably with experimental results and to be slightly superior to the results produced by conventional structural analysis.

INTRODUCTION

The derivation of a mathematical model of a complex structure, such as a launch vehicle or spacecraft, suitable for dynamic, transient-response analysis is a difficult task and much effort has been expended in developing improved capabilities in the area of structural response analysis. Most methods require detailed knowledge of the physical and geometrical properties of the structure from which mathematical idealizations are used to construct a lumped-parameter analytical model using a finite-element approach. The analytical model in the form of mass and stiffness matrices corresponding to the selected coordinates can then be solved to determine the natural modes of vibration and the forced response of the structure.

---

*Some of the information presented herein was previously included in a paper "Identification of Complex Structures Using Near-Resonance Testing," presented at the 38th Shock and Vibration Symposium, St. Louis, Missouri, May 1 and 2, 1968.

In most cases the structural analyst must rely on experimental data from static and dynamic tests as a basis for modifying and verifying the derived analytical model. Also, in the derivation of the analytical model of a complex structure, the analyst must provide maximum capability for analyzing in detail problems which may be specified only at a later time. Thus, the entire structure must be treated to the same level of detail and, in general, the number and accuracy of the vibration modes determined should be adequate for any future response analysis. Unfortunately, these attempts to provide analytical capability for a wide variety of problems frequently result in insufficient information when a specific problem of interest has been completely described.

Therefore, the desirability of simple techniques for generating an analytical model derived solely from experimental data and tailored to a unique dynamic response problem involving a specific input-output transmission path for the structure is suggested. The techniques of system identification in which both the required modal equations and their coefficients are determined from experimental data seem to be well suited to the attainment of this goal.

The purpose of this paper is to present a simple technique for experimentally determining an acceptable set of equations of motion for a space-vehicle structure. This system identification approach, although it yields the equations of motion, does not involve a detailed structural analysis of the system. It relies solely on the experimental determination of the steady-state response of the structure to a sinusoidally varying input force for a few frequencies near each important structural resonance and on the usual assumptions regarding the behavior of lightly damped, linear structures.

SYMBOLS

$[C]$ system viscous damping matrix; symmetric, nonnegative definite

$\left[\ddots\ \overline{C}\ \ddots\right]$ diagonal modal damping matrix

$\{F(t)\}$ system-forcing-function vector

F_i amplitude of $F_i \sin \omega t$

$F_i(t)$ arbitrary external point force applied at i

f frequency

i,k input and output points, respectively

j	designates specific modes
$[K]$	system stiffness matrix; symmetric, nonnegative definite
$\left[\diagdown \bar{K} \diagdown\right]$	diagonal modal stiffness matrix
$[M]$	system mass matrix; symmetric, positive definite
$\left[\diagdown \bar{M} \diagdown\right]$	diagonal modal mass matrix
$m_{ik}^{(j)}, c_{ik}^{(j)}, k_{ik}^{(j)}$	effective mass, damping, and stiffness for the i to k input-output path in jth mode (j = 1,2,. . .,p)
m_j, c_j, k_j	jth modal mass, damping, and stiffness
p	total number of modes
$\{q\}$	normal coordinates defined by $\{X\} = [\psi]\{q\}$
q_j	jth element of $\{q\}$
$\{X\}$	system coordinate vector
$\{X\}^{(j)}$	system coordinate vector due only to response in jth mode
X_k	amplitude of steady-state displacement response at k
x_k	kth system coordinate; an element of $\{X\}$
$x_k^{(j)}$	kth element of $\{X\}^{(j)}$
θ_{ik}	phase angle between response and input force for the i,k path
$\mu_{ik}^{(j)}$	effective percent of critical damping in jth mode
$\varphi_i^{(j)}, \varphi_k^{(j)}$	ith and kth elements of $\{\varphi\}^{(j)}$

$\{\varphi\}^{(j)}$ jth modal vector obtained from $\left[[K] - \omega_j^2[M]\right]\{X\} = 0$

$[\psi]$ matrix of modal vectors $\{\varphi\}^{(j)}$ as columns

ω circular frequency

ω_j jth resonant circular frequency

$[\ ]^T$ transpose of matrix

A dot over a symbol denotes differentiation with respect to time.

THEORY

The starting point for the development of the identification technique of this paper is in the mechanics of lightly damped, linear systems. The class of structures for which the technique is proposed is assumed to possess the following somewhat qualitative features which are stated in the form of assumptions and are basic to the ensuing development:

(1) Light damping typical of a space vehicle without damping specifically designed into the structure.

(2) The modes of interest are sufficiently uncoupled in the velocity terms and separated in frequency so that a single-degree-of-freedom analysis (one second-order differential equation with constant coefficients) is adequate to represent the steady-state response of the system in a frequency band near the resonant frequency in a mode of interest.

These basic assumptions are intended to imply that the steady-state response in each vibration mode of interest is not significantly affected by any other mode and that each mode can be isolated and individually exploited as discussed in detail in references 1 to 4.

With these assumptions as a background, the proposed identification technique and the supporting analytical arguments are now developed.

General Theory

The equations of motion for an N-degree-of-freedom linear dynamic system may be written (ref. 5)

$$[M]\{\ddot{X}\} + [C]\{\dot{X}\} + [K]\{X\} = \{F(t)\} \tag{1}$$

The transformation

$$\{X\} = [\psi]\{q\} \tag{2}$$

where

$$x_k = \sum_j \varphi_k^{(j)} q_j \tag{3}$$

is assumed to produce uncoupled equations in terms of the normal coordinates q so that

$$\left[\overline{M}\right]\{\ddot{q}\} + \left[\overline{C}\right]\{\dot{q}\} + \left[\overline{K}\right]\{q\} = [\psi]^T\{F(t)\} \tag{4}$$

where

$$\left[\overline{M}\right] = [\psi]^T[M][\psi]$$

$$\left[\overline{C}\right] = [\psi]^T[C][\psi]$$

$$\left[\overline{K}\right] = [\psi]^T[K][\psi]$$

The equation for the jth normal coordinate is

$$m_j\ddot{q}_j + c_j\dot{q}_j + k_jq_j = \sum_i \varphi_i^{(j)} F_i(t) \tag{5}$$

For only one external forcing function applied at i, equation (5) becomes

$$m_j\ddot{q}_j + c_j\dot{q}_j + k_jq_j = \varphi_i^{(j)} F_i(t) \tag{6}$$

Near-Resonant Response

Equation (2) may be written

$$\{X\} = \sum_j \{\varphi\}^{(j)} q_j$$

so that the response in the jth mode is

$$\{X\}^{(j)} = \{\varphi\}^{(j)} q_j \tag{7}$$

or

$$x_k^{(j)} = \varphi_k^{(j)} q_j \tag{8}$$

and

$$q_j = \frac{x_k^{(j)}}{\varphi_k^{(j)}} \tag{9}$$

Substituting equation (9) into equation (6) and dividing by $\varphi_i^{(j)}$ yields

$$\left(\frac{m_j}{\varphi_i^{(j)} \varphi_k^{(j)}}\right) \ddot{x}_k^{(j)} + \left(\frac{c_j}{\varphi_i^{(j)} \varphi_k^{(j)}}\right) \dot{x}_k^{(j)} + \left(\frac{k_j}{\varphi_i^{(j)} \varphi_k^{(j)}}\right) x_k^{(j)} = F_i(t) \tag{10}$$

or

$$m_{ik}^{(j)} \ddot{x}_k^{(j)} + c_{ik}^{(j)} \dot{x}_k^{(j)} + k_{ik}^{(j)} x_k^{(j)} = F_i(t) \tag{11}$$

where

$$m_{ik}^{(j)} = \frac{m_j}{\varphi_i^{(j)} \varphi_k^{(j)}}$$

$$c_{ik}^{(j)} = \frac{c_j}{\varphi_i^{(j)} \varphi_k^{(j)}}$$

$$k_{ik}^{(j)} = \frac{k_j}{\varphi_i^{(j)} \varphi_k^{(j)}}$$

Note that these coefficients are, respectively, positive or negative depending on whether the responses at $\varphi_i^{(j)}$ and $\varphi_k^{(j)}$ are in phase or out of phase.

The significance of equation (11) is that it represents the response of the jth mode at point k due to forcing at point i. Also, the derivation of equation (11) has not placed any restrictions on the forcing function at i. In fact, $F_i(t)$ is an arbitrary, external, point forcing function.

Identification Approach

When $F_i(t) = F_i \sin \omega t$ with ω near ω_j, assumption (2) implies that only one equation with constant coefficients of the form of equation (11) is required to represent the system response. In this case, the steady-state or particular solution of equation (11) is of the form:

$$x = X \sin(\omega t - \theta) \tag{12}$$

Substituting equation (12) into equation (11) and solving for the coefficients m_{ik}, c_{ik}, and k_{ik} results in

$$k_{ik}^{(j)} = m_{ik}^{(j)} \omega^2 + \frac{F_i}{X_k} \cos \theta_{ik} \tag{13}$$

and

$$c_{ik}^{(j)} = \frac{F_i}{\omega X_k} \sin \theta_{ik} \tag{14}$$

If one set of values of ω, F_i, X_k, and θ_{ik} for equation (14) and two sets for equation (13) are known, the coefficients of equation (11) may be computed.

Response to Arbitrary Force

The total system response at k due to any time-dependent force $F_i(t)$ at i is found by superposition of the solutions of each of the set of the following equations:

$$
\left.
\begin{aligned}
m_{ik}^{(1)}\ddot{x}_k^{(1)} + c_{ik}^{(1)}\dot{x}_k^{(1)} + k_{ik}^{(1)}x_k^{(1)} &= F_i(t) \\
&\vdots \\
m_{ik}^{(j)}\ddot{x}_k^{(j)} + c_{ik}^{(j)}\dot{x}_k^{(j)} + k_{ik}^{(j)}x_k^{(j)} &= F_i(t) \\
&\vdots \\
m_{ik}^{(p)}\ddot{x}_k^{(p)} + c_{ik}^{(p)}\dot{x}_k^{(p)} + k_{ik}^{(p)}x_k^{(p)} &= F_i(t)
\end{aligned}
\right\} \tag{15}
$$

and is given if equations (3) and (8) are used as

$$
x_k = \sum_{j=1}^{p} x_k^{(j)} \tag{16}
$$

Note that in order to obtain the solution, the initial conditions for equations (15) must be known. In general, the initial conditions are

$$
\left.
\begin{aligned}
x_k^{(j)}(0) &= \varphi_k^{(j)} q_j(0) \qquad (j = 1,2,\ldots,p) \\
\dot{x}_k^{(j)}(0) &= \varphi_k^{(j)} \dot{q}_j(0) \qquad (j = 1,2,\ldots,p)
\end{aligned}
\right\} \tag{17}
$$

For zero initial conditions, equations (17) become

$$
\left.
\begin{aligned}
x_k^{(j)}(0) &= 0 \qquad (j = 1,2,\ldots,p) \\
\dot{x}_k^{(j)}(0) &= 0 \qquad (j = 1,2,\ldots,p)
\end{aligned}
\right\} \tag{18}
$$

If equations (18) are satisfied, the total response of point k to an arbitrary forcing function at point i can be determined without any knowledge of the quantities $\varphi_k^{(j)}$. For nonzero initial conditions, the matrix $[\psi]$ must be determined. In this report, the problems involving transient forcing functions have zero initial conditions.

Computer Experiments for Sinusoidal Inputs

A controlled computer experiment was conducted in order to test the accuracy of the proposed identification method. For convenience, equations (15) were written as

$$\left.\begin{aligned} \ddot{x}_k^{(1)} + 2\mu_{ik}^{(1)}\omega_1\dot{x}_k^{(1)} + \omega_1^2 x_k^{(1)} &= \frac{1}{m_{ik}^{(1)}} F_i(t) \\ \cdot \quad \cdot \quad \cdot \quad \cdot & \\ \cdot \quad \cdot \quad \cdot \quad \cdot & \\ \cdot \quad \cdot \quad \cdot \quad \cdot & \\ \ddot{x}_k^{(p)} + 2\mu_{ik}^{(p)}\omega_p\dot{x}_k^{(p)} + \omega_p^2 x_k^{(p)} &= \frac{1}{m_{ik}^{(p)}} F_i(t) \end{aligned}\right\} \tag{19}$$

A set of coefficients of equations (19) was assumed and an exact numerical solution was generated for a sinusoidal forcing function. The computed response obtained was then "corrupted" by the addition of random errors and the coefficients $m_{ik}^{(j)}$, $c_{ik}^{(j)}$, and $k_{ik}^{(j)}$ were computed from equations (13) and (14) for four or five frequencies near each resonance. The value of $c_{ik}^{(j)}$ for each point was computed from equation (14). The values of $m_{ik}^{(j)}$ and $k_{ik}^{(j)}$ were computed from equation (13), which was considered as a pair of simultaneous equations for slightly different near-resonant values of ω. The values of $m_{ik}^{(j)}$, $c_{ik}^{(j)}$, and $k_{ik}^{(j)}$ so determined were found to vary, depending upon which pair of points were used in solving equations (13) and (14). These results mean that no single set of values of $m_{ik}^{(j)}$, $c_{ik}^{(j)}$, and $k_{ik}^{(j)}$ will produce a frequency-response curve which passes exactly through all the points of the corrupted data. An obvious way to circumvent this difficulty is to use a least-squares fit. However, the resulting equations were found to be ill-conditioned in all cases which were attempted. For this reason, the different values which were obtained were simply averaged. The results of using this averaging technique indicated that errors of up to ±10 percent in F_i/X_k and $\pm 10^o$ in θ_{ik} can be tolerated by this identifier when applied to systems which satisfy the basic assumptions of this paper. Since it was felt that the accuracy of experimental data fell within these limits, identification of the 1/10-scale and 1/40-scale models was attempted.

EXPERIMENTAL PROCEDURE

The Langley 1/10-scale and 1/40-scale models of the Apollo-Saturn V launch vehicle are shown in figures 1 and 2 and a schematic diagram of both models is presented in figure 3. The 1/10-scale model is fully described in reference 6.

1/10-Scale Model

The 1/10-scale model was complete in the lift-off structural configuration, but was empty of simulated propellants. The boundary conditions were cantilevered-free. A constant-frequency, transverse, sinusoidally varying input force of about 15N was applied in the pitch plane through a strain-gage type of force gage at station 386 and the displacements at stations 418 (the tip of the escape tower), 377, and 282 were measured by using a contacting, cantilever, strain-gage beam. The strain-gage displacement transducers had natural frequencies of the order of 60 Hz and were used within their flat-response regime. The signals from the force and the displacement transducers were processed through a balancing bridge, a differential amplifier, and a dc isolation amplifier and were then recorded together with the calibration signals on a frequency-modulated (FM) analog tape recorder. The selection of both strain-gage force and displacement transducers with both signals processed through similar parallel electronics was to minimize the relative phase shift and thus assure the accurate determination of phase angle θ_{ik} for use in equations (13) and (14).

1/40-Scale Model

The 1/40-scale model was also complete in the lift-off structural configuration. Propellant loading corresponded to first-stage burnout and the boundary conditions simulated were free-free. A constant-frequency transverse, sinusoidally varying input force of about 2N was applied in the pitch plane through a crystal-type force gage alternately at stations 0 and 42 and the acceleration responses were measured with crystal accelerometers at several model stations. Transient responses for the same transmission paths were also obtained by tapping the model at stations 0 and 42. The crystal transducers were used with this model in order to demonstrate that satisfactory results could be obtained from either of the two different instrumentation schemes. The signals from the force gage and accelerometers were processed through similar conditioning equipment to minimize relative phase shift and, together with calibration signals, were recorded on an FM tape recorder.

Data Reduction

The experimental analog data for input force and displacement or acceleration response were converted to digital data and then were filtered by using a 24-point-per-cycle Fourier analysis from which the numerical amplitudes of the fundamental components of the input force and of the displacement and acceleration responses and the input-response phase angles θ_{ik} were computed.

Solution for Coefficients

The digitized experimental data F_i, θ_{ik}, and X_k or $\ddot{x}_k/\omega^2$ corresponding to a near-resonant value of ω were used as described to determine the average values of $m_{ik}^{(j)}$, $c_{ik}^{(j)}$, and $k_{ik}^{(j)}$ for each significant mode for each of the selected input-response paths for each model. These results are listed as coefficients of equation (19) in tables I and II. Typical first mode (j = 1) values for station 377 response of the 1/10-scale model are as follows:

Frequency, f, Hz, for –		Coefficients of equation (11)			Coefficients of equations (19)		
Equation (14)	Equation (13)	$m_{ik}^{(1)}$, kg	$c_{ik}^{(1)}$, $\frac{\text{N-sec}}{\text{m}}$	$k_{ik}^{(1)}$, $\frac{\text{N}}{\text{m}}$	$2\mu_{ik}\omega_1 = \frac{c_{ik}^{(1)}}{m_{ik}^{(1)}}$, rad/sec	$\omega_1^2 = \frac{k_{ik}^{(1)}}{m_{ik}^{(1)}}$, rad/sec	$\frac{1}{m_{ik}^{(1)}}$, $\frac{1}{\text{kg}}$
4.52	4.52; 4.72	60.93	25.53	53 400	0.4190	876.4	0.0164
4.72	4.52; 4.99	59.21	28.28	51 870	.4776	876.0	.0169
4.99	4.72; 4.99	57.98	28.21	50 800	.4865	876.2	.0172

It should be mentioned that the system identification method presented herein has been devised specifically for the exploitation of particular input-output transmission paths. No attempt has been made to obtain either resonant response or normal mode data which are valid for the entire structure. For example, in table I the natural frequencies for the second mode are slightly different for different transmission paths. Thus, caution must be exercised in using the data for a particular transmission path, possibly together with other information such as resonant response or normal mode data, to infer the values of the parameters for other transmission paths.

STRUCTURAL ANALYSIS

A structural analysis of the 1/40-scale model was conducted in order to obtain data for comparison purposes. The 1/40-scale model was treated as a beam with lumped masses and finite elastic elements. Complete details of the procedure which was followed are presented in references 7 and 8. Mass and stiffness matrices were obtained for the 1/40-scale model complete in the lift-off structural configuration. The boundary conditions were free-free. Simulated propellant mass was then removed to correspond to the propellant loading at first-stage burnout. The final mass and stiffness matrices represented the vehicle as a system with 23 degrees of freedom. A standard numerical

eigenvalue routine was used to compute the mode shapes and frequencies; these values were then used to compute the transient response.

RESULTS AND DISCUSSION

Comparisons of the identification and experimental frequency responses for the two models are presented in figures 4 to 6.

1/10-Scale Results

The frequency-response results for the 1/10-scale model plotted as the variation of the response ratio $\left|\frac{X_k}{F_i}\right|$ with frequency are shown in figure 4. The particular solutions of equations (19) were obtained for $F_i(t) = \sin \omega t$ $(i = 386)$ for $0 \leqq \frac{\omega}{2\pi} \leqq 30$ by using the coefficients given in table I. The frequency response at stations 418, 377, and 282 were then obtained by using equation (16), which it should be noted includes both modal amplitude and phase. For example,

$$x_{418} = x_{418}^{(1)} + x_{418}^{(2)} + x_{418}^{(3)}$$

the amplitude of which is plotted in figure 4.

1/40-Scale Results

The frequency-response results for the 1/40-scale model are shown in figures 5 and 6. The frequency-response solutions shown in these figures for forcing first at station 0 and then at station 42 were computed by using equations (16) and (19) and the coefficients given in table II. For example, for the steady-state response at station 102.9 due to forcing at station 42

$$\ddot{x}_{102.9}^{(1)} + 3.14\dot{x}_{102.9}^{(1)} + 69\ 530x_{102.9}^{(1)} = -0.0577 \sin \omega t$$

$$\ddot{x}_{102.9}^{(2)} + 4.54\dot{x}_{102.9}^{(2)} + 289\ 300x_{102.9}^{(2)} = 0.0925 \sin \omega t$$

$$\ddot{x}_{102.9}^{(3)} + 13.71\dot{x}_{102.9}^{(3)} + 681\ 160x_{102.9}^{(3)} = -0.0697 \sin \omega t$$

$$\ddot{x}_{102.9}^{(4)} + 26.25\dot{x}_{102.9}^{(4)} + 929\ 870x_{102.9}^{(4)} = -0.0668 \sin \omega t$$

and

$$x_{102.9} = x^{(1)}_{102.9} + x^{(2)}_{102.9} + x^{(3)}_{102.9} + x^{(4)}_{102.9}$$

where the absolute values of amplitude are plotted in figures 5 and 6.

The transient-response results for the 1/40-scale model are shown in figures 7 and 8. Transient responses were obtained experimentally for the same transmission paths for which frequency-response data are shown in figures 5 and 6 and for which identified equations of motion had been obtained. The transient responses were computed by numerical integration of the identified equations of motion (eq. (19)) by using as a forcing function the experimentally measured input transient force. Equation (16) was used to compute the total response.

Frequency-Response Results

The identification results for both models agree very favorably with the experimental response data. In addition to the amplitude agreement shown in figures 4 to 6, the associated phase angles $\angle x_k/F_i$ also agree, usually to within 5^o to 10^o. Therefore, it is felt that for both models and for the input-response paths investigated, systems of equations suitable for computing the response to an arbitrary forcing function have been obtained.

The experience thus far also indicates that for the class of systems considered in this paper, an identification scheme based on requiring coincidence of frequency-response amplitudes only will produce basically the same results as if both amplitude and phase information were employed. (This point is discussed in detail in chapter 6 of ref. 9.) This fact can be useful because, in general, some obvious adjustments of the identified parameters to give better results based on amplitude comparison is usually possible. In figures 4 to 6, all except figures 5(b) and 5(c) indicate the results that were achieved by using the method of this paper without any such adjustment of parameters. However, parameters can easily be selected to produce an improved agreement in any of the amplitude plots of these figures if desired. The resulting phase differences are small but always are improvements. An example of the effect of these adjustments on the amplitude and phase angle is shown in figures 9 and 10, respectively, for the data presented in figure 5(b). The adjustments were selected on the basis of producing a better amplitude comparison; also these adjustments resulted in improvements in the phase plots. Therefore, it is felt that refinement of the identified equations to produce improved amplitude agreement is permissible and desirable.

In this connection, the uniqueness of the identified equations has not been rigorously established. It is, however, felt that amplitude agreement as shown in figures 4 to 6 together with a phase agreement to within 5^{o} to 10^{o} constitutes sufficient conditions for a system identification adequate for all engineering purposes.

Thus, the equations of motion have been obtained without a detailed structural idealization and associated analytical model. The modes that actually contributed to the response were immediately identified as the only ones observable for a given input-response path. This identification of the modes obviated the usual concern over the problem of including the appropriate number of vibratory modes of the structure.

It should be pointed out that in figure 5(d), a fourth mode was inadvertently omitted. The presence of this mode at $f = 165$ Hz was later indicated by examination of slow sine sweep plots taken in connection with references 7 and 8. Since the model was no longer available, no further testing was attempted.

Transient-Response Results

Once the equations of motion for a structure have been identified, the transient response to an arbitrary force can be computed with confidence. In this connection, rigid body modes, if required, can be calculated from model drawings or can be experimentally determined. Results of transient tests with the 1/40-scale model produced excellent agreement between the acceleration response computed by using the identified equations and the experimental transient acceleration responses. For example, comparisons of identification and experimental transient acceleration and displacement responses for the 1/40-scale model are shown in figures 7 and 8. The coefficients used in computing the acceleration response as predicted with the use of the system identification results are given in table II. (See figs. 5 and 6.) In addition, the two zero-frequency rigid body modes required were analytically determined from model drawings; their inclusion resulted in two additional equations of motion. The complete system of equations was numerically integrated by using the measured values of the transient input which was applied at stations 0 and 42 of the model. The identified equations predict transient acceleration and displacement responses which are in good agreement with the experimentally determined response. The results of figures 7 and 8 are especially important because they demonstrate the ability of the identified equations to predict accurately the response to an input of a different character than was used for their derivation.

The acceleration response shown in figure 7(c) indicates the effect of neglecting to identify the fourth mode for this transmission path. (See fig. 5(d).) The transient experimental results contain an oscillatory frequency in the neighborhood of the frequency which was omitted from the representation. This mode was included in the transmission

path for figure 8(c) (see fig. 6(b)) and the transient-response comparison is clearly improved. Thus, it appears that if a particular mode is neglected in the identification of a system, that mode will be filtered from the calculated response without the loss of other significant information.

Transient Response by Structural Analysis

In order to obtain further evaluation of the method presented in this report, the transient acceleration responses at station 102.9 for two transient force input locations were computed by using the mathematical model derived in reference 7. A comparison of the experimental, system identification, and the analytical transient acceleration responses for each of these two cases is shown in figure 11.

The results using the structural analysis incorporated the 23 undamped modes produced by the mathematical model. The system identification results incorporated two undamped rigid body modes and three and four damped flexure modes, respectively, for figures 11(a) and 11(b). Setting damping equal to zero in the identified equations results, however, in no change in the computed transient response over the time interval shown.

Figure 11 indicates that the identified equations produced transient-response results which are slightly superior to the results produced by conventional structural analysis.

CONCLUDING REMARKS

A technique for determining the equations of motion of a complex structure has been presented. Both the number of the essential degrees of freedom and the coefficients of the equations are determined by the procedure which is applicable to a large class of aerospace structures and other structures. The procedure requires that good quality experimental frequency-response data be obtained for the significant resonances associated with specified input-response paths. The strength of the method is that it does not require prior knowledge of the system degrees of freedom. This knowledge is determined as part of the procedure.

This identification procedure should be advantageous when the dynamical equations of motion for an existing structure are desired. For example, the procedure of this paper may be very useful if the available resources are not sufficient to allow the formulation and verification of a detailed analytical model of an existing structure or if only sinusoidal test equipment is available, but transient response data are required. In this connection, both displacement and acceleration sensing and conditioning instrumentation were found to be capable of producing data adequate for satisfactory system identification.

In particular, the equations for a 1/40-scale model of the Apollo-Saturn V launch vehicle which were identified by using the experimental data for sinusoidal inputs were shown to predict adequately the system acceleration response to an arbitrary transient force. In fact, the results were somewhat superior to a 23-degree-of-freedom finite-element analytical model based on structural parameters.

It is felt that for the class of structures considered in this paper, coincidence of the identified and experimental frequency-response amplitudes constitutes a sufficient condition for a satisfactory identification. This suggests that refinement of the initial identification results to produce improved amplitude agreement is desirable and may be useful in the formulation of an identifier that does not require explicit experimental phase information.

Langley Research Center,
National Aeronautics and Space Administration,
Langley Station, Hampton, Va., November 15, 1968,
124-08-05-02-23.

REFERENCES

1. Plunkett, Robert: Semi-Graphical Method for Plotting Vibration Response Curves. Proceedings of the Second U.S. National Congress of Applied Mechanics, Amer. Soc. Mech. Eng., c.1955, pp. 121-126.

2. Thorn, Richard P.; and Church, Austin H.: Simplified Vibration Analysis by Mobility and Impedance Methods. Mach. Design, c.1959, 1960.

3. Raney, J. P.: Analog Computer Solution for Transverse Vibrations of a Uniform Beam With Damped, Flexible, Massive End Restraints. Developments in Theoretical and Applied Mechanics, Vol. 1, Plenum Press, 1963, pp. 87-99.

4. Howlett, James T.; and Raney, John P.: New Approach for Evaluating Transient Loads for Environmental Testing of Spacecraft. Shock Vib. Bull., Bull. 36, Pt. 2, U.S. Dep. Def., Jan. 1967, pp. 97-106.

5. Caughey, T. K.; and O'Kelley, M. E. J.: Classical Normal Modes in Damped Linear Dynamic Systems. Trans. ASME, Ser. E: J. Appl. Mech., vol. 32, no. 3, Sept. 1965, pp. 583-588.

6. Leadbetter, Sumner A.; Leonard, H. Wayne; and Brock, E. John, Jr.: Design and Fabrication Considerations for a 1/10-Scale Replica Model of the Apollo/Saturn V. NASA TN D-4138, 1967.

7. Steeves, Earl C.; and Catherines, John J.: Lateral Vibration Characteristics of a 1/40-Scale Dynamic Model of Apollo-Saturn V Launch Vehicle. NASA TN D-4872, 1968.

8. Adelman, Howard M.; and Steeves, Earl C.: Vibration Analysis of a 1/40-Scale Dynamic Model of Saturn V—Launch-Platform—Umbilical-Tower Configuration. NASA TN D-4871, 1968.

9. Truxal, John G.: Automatic Feedback Control System Synthesis. McGraw-Hill Book Co., Inc., 1955.

TABLE I.- IDENTIFIED VALUES OF THE COEFFICIENTS OF EQUATIONS (19) FOR THE 1/10-SCALE MODEL

[All stages empty, cantilevered-free]

Coefficient	Identified values for input-output path i;k						
	386; 418 for mode –			386; 377 for mode –		386; 282 for mode –	
	1	2	3	1	2	1	2
$2\mu_{ik}^{(j)}\omega_j$, rad/sec . . .	0.472	4.19	15.4	0.477	3.40	0.479	2.85
ω_j^2, $(\text{rad/sec})^2$	877	9240	28 360	876	8860	877	9350
$\frac{1}{m_{ik}^{(j)}}, \frac{1}{kg}$	0.0222	0.0514	-0.0277	0.0168	0.0131	0.00793	-0.0110

TABLE II.- IDENTIFIED VALUES OF THE COEFFICIENTS OF EQUATIONS (19) FOR 1/40-SCALE MODEL

[First stage empty, free-free]

Coefficient	Identified values for input-output path i;k					
	0; 102.9 for mode –			0; -2.7 for mode –		
	1	2	3	1	2	3
$2\mu_{ik}^{(j)}\omega_j$, rad/sec . . .	4.00	6.76	13.90	2.76	5.20	60.0
ω_j^2, $(\text{rad/sec})^2$	68 900	288 000	683 000	69 000	288 000	680 000
$\frac{1}{m_{ik}^{(j)}}, \frac{1}{\text{kg}}$	0.223	-0.164	0.0577	0.0392	0.0185	0.0582

Coefficient	Identified values for input-output path i;k					
	0; 81.5 for mode –			0; 9.3 for mode –		
	1	2	3	1	2	3
$2\mu_{ik}^{(j)}\omega_j$, rad/sec . . .	3.18	11.9	33.4	3.0	10.0	Negligible third-mode response for this path
ω_j^2, $(\text{rad/sec})^2$	68 800	289 000	683 000	69 000	289 000	
$\frac{1}{m_{ik}^{(j)}}, \frac{1}{\text{kg}}$	0.0116	0.0166	-0.00736	0.0120	0.00805	

TABLE II.- IDENTIFIED VALUES OF THE COEFFICIENTS OF EQUATIONS (19) FOR 1/40-SCALE MODEL – Concluded

Coefficient	Identified values for input-output path i;k							
	42; 102.9 for mode –				42; -2.7 for mode –			
	1	2	3	4	1	2	3	4
$2\mu_{ik}^{(j)}\omega_j$, rad/sec . . .	3.14	4.54	13.71	26.25	4.2	2.68	30.60	20.12
ω_j^2, $(\text{rad/sec})^2$	69 530	289 300	681 160	929 870	69 700	287 100	691 650	933 400
$\frac{1}{m_{ik}^{(j)}}$, $\frac{1}{\text{kg}}$	-0.0577	0.0925	-0.0697	-0.0668	-0.0161	-0.0128	-0.00782	-0.0154

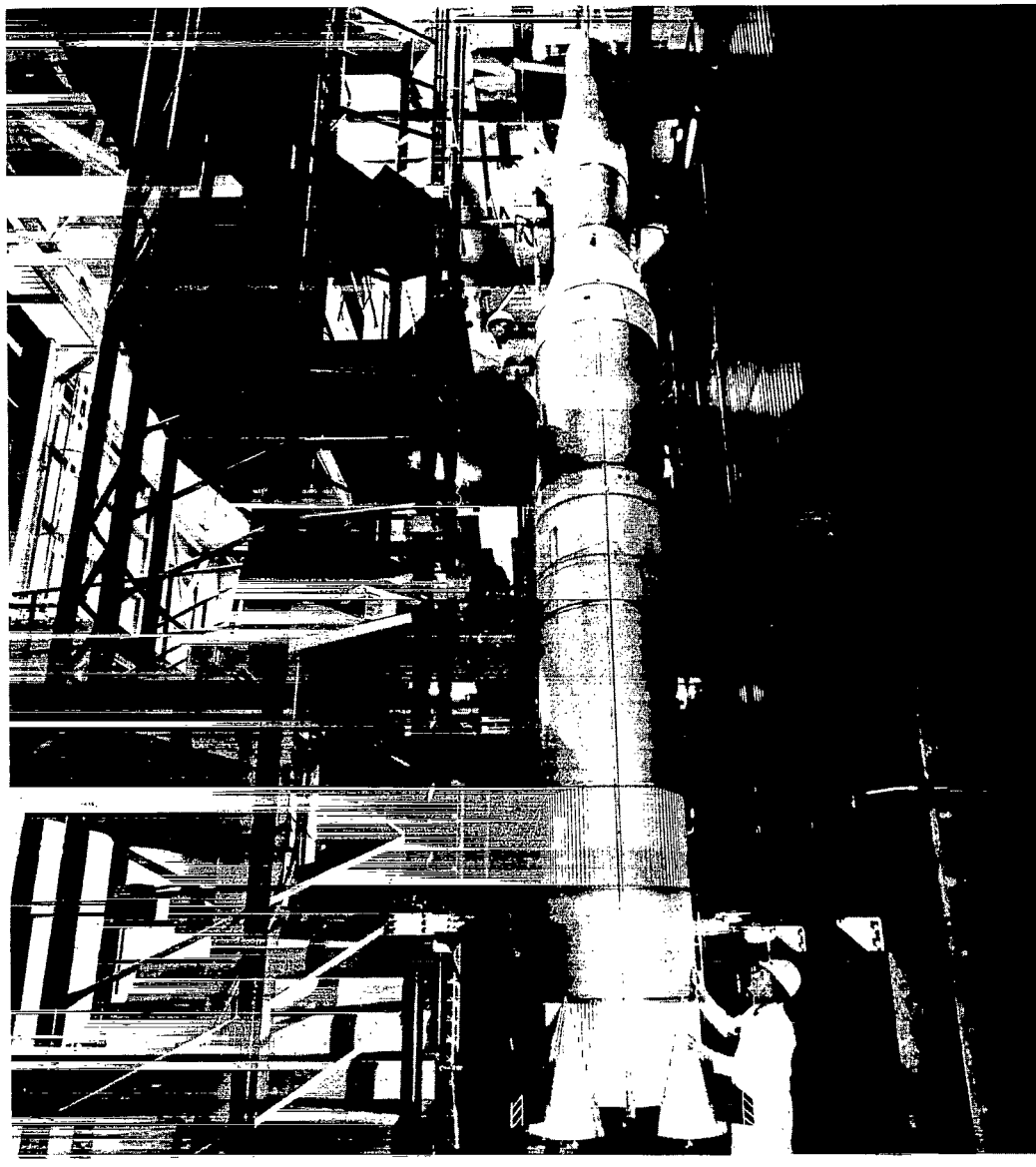

Figure 1.- 1/10-scale Apollo-Saturn V model. L-68-10,010

Figure 2.- 1/40-scale Apollo-Saturn V model. L-68-10,011

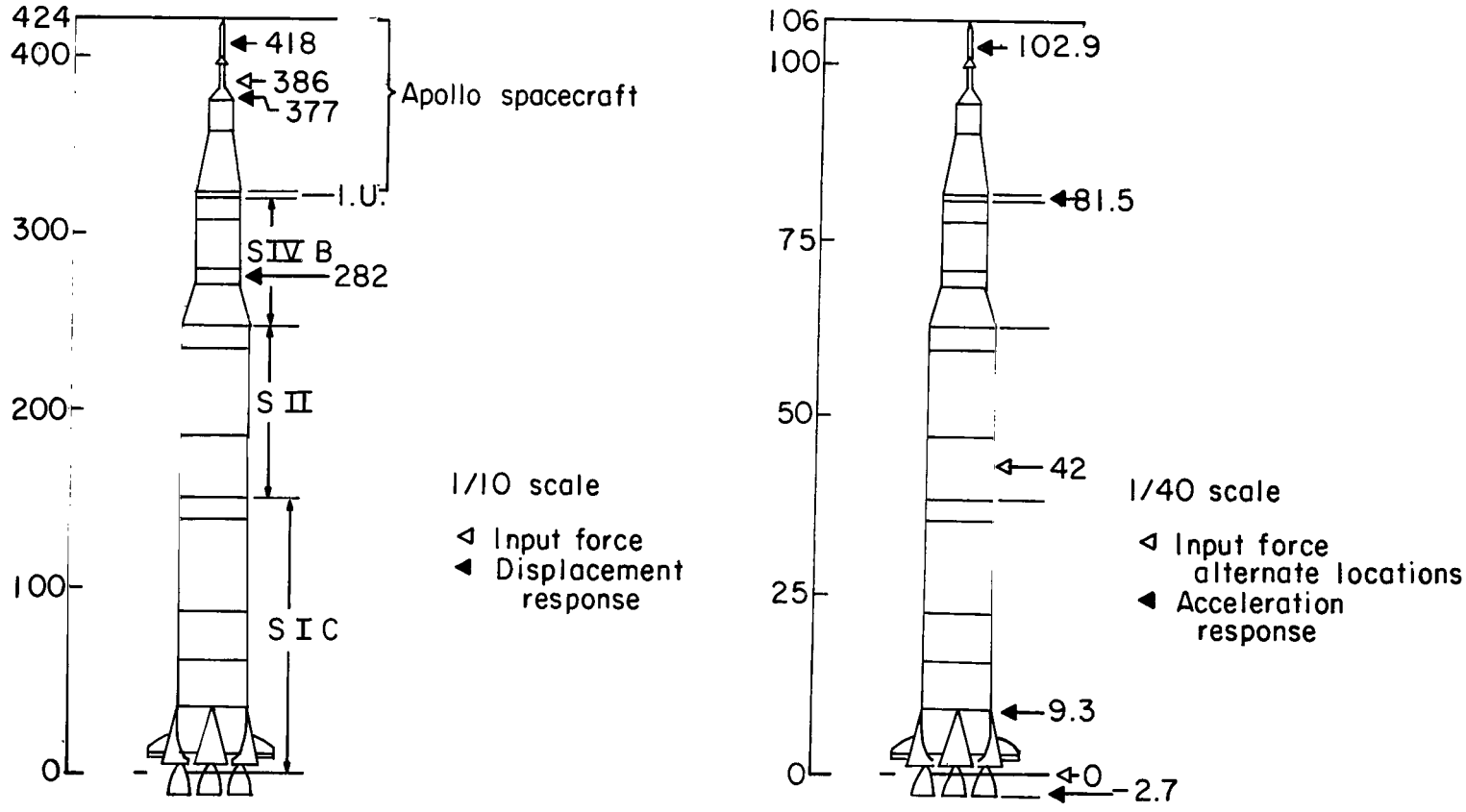

Figure 3.- Schematic diagram of Apollo-Saturn V models. (I.U. designates instrument unit.)

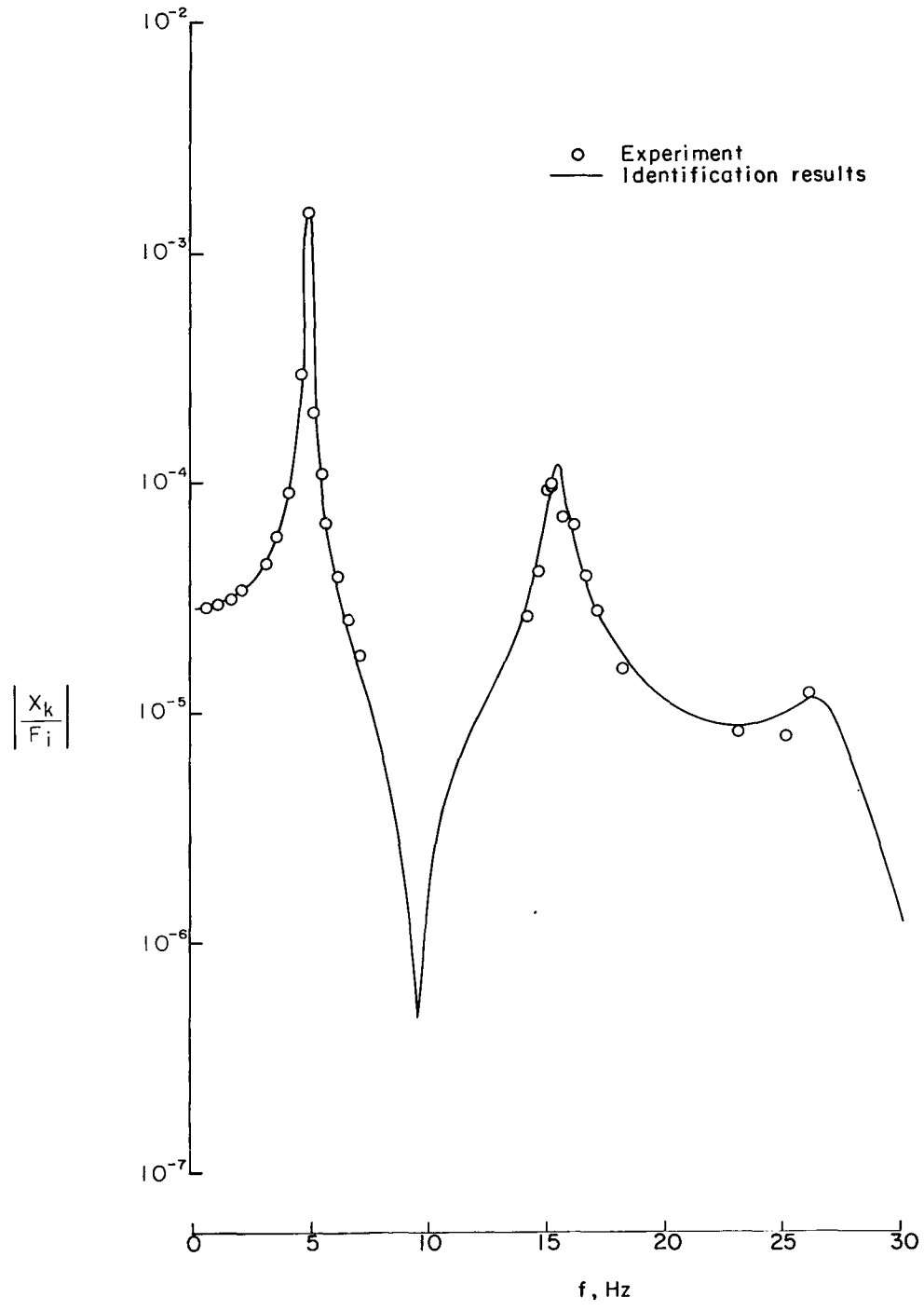

(a) Response at station k = 418.

Figure 4.- Comparison of identification results with experimental frequency response for 1/10-scale model forced at station i = 386.

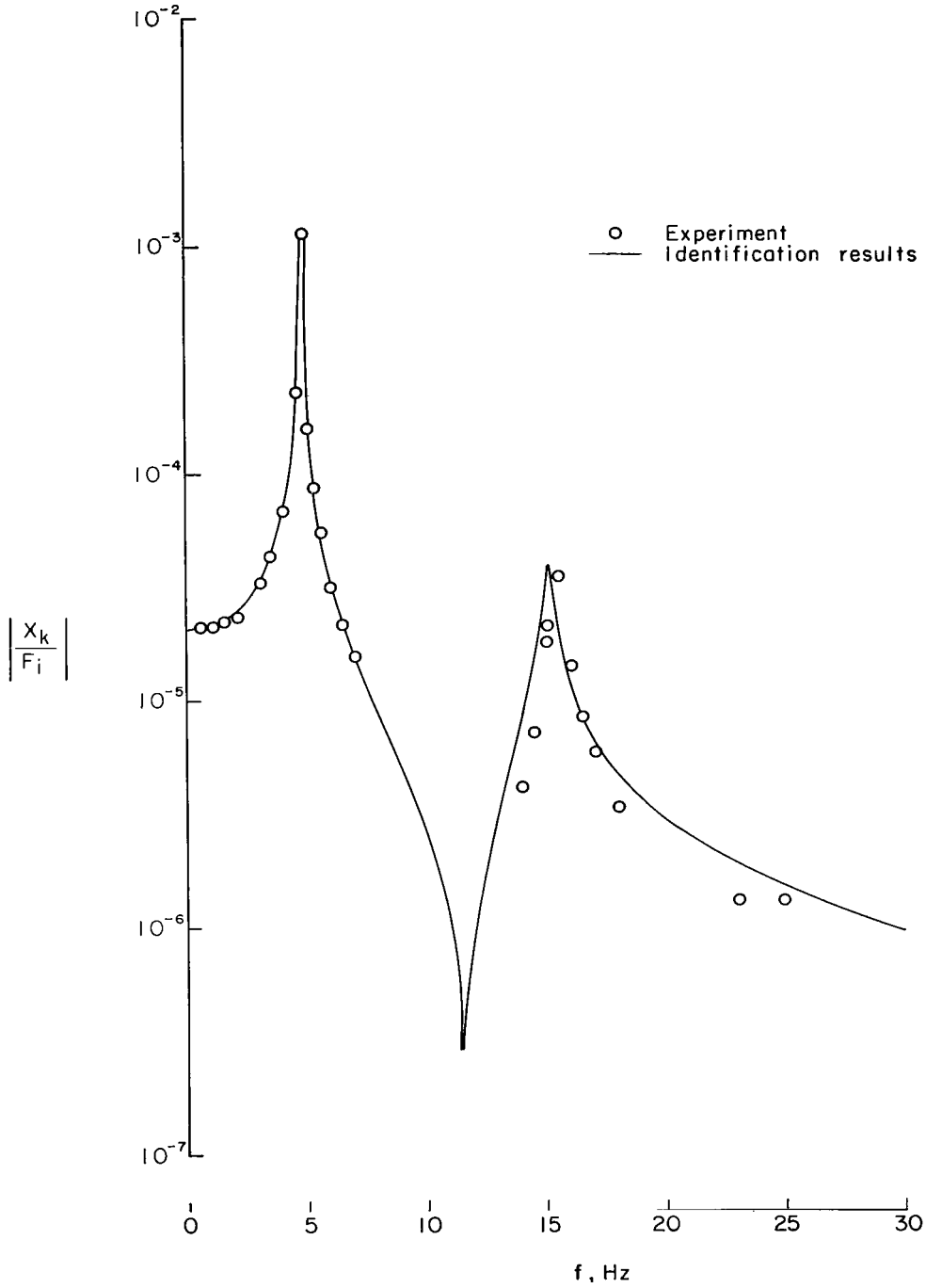

(b) Response at station k = 377.

Figure 4.- Continued.

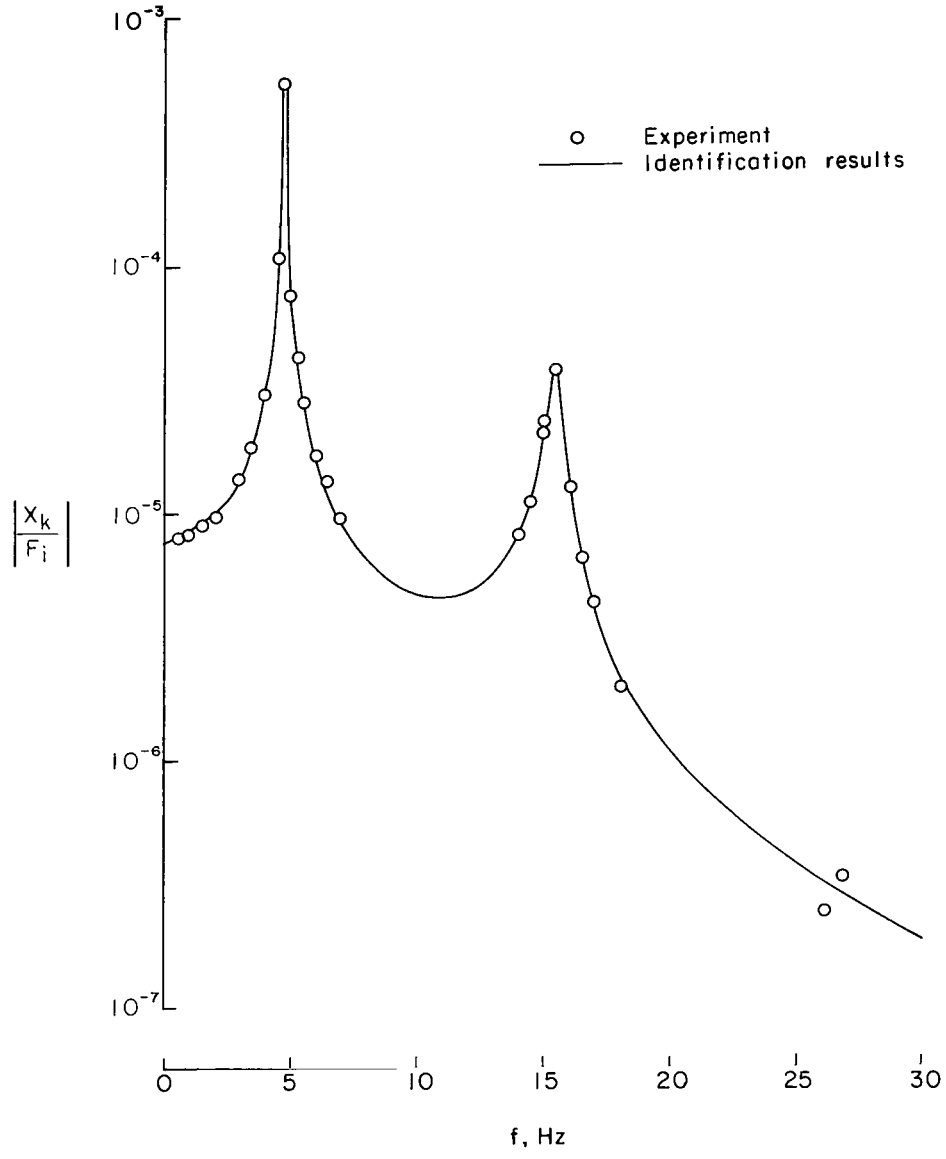

(c) Response at station k = 282.

Figure 4.- Concluded.

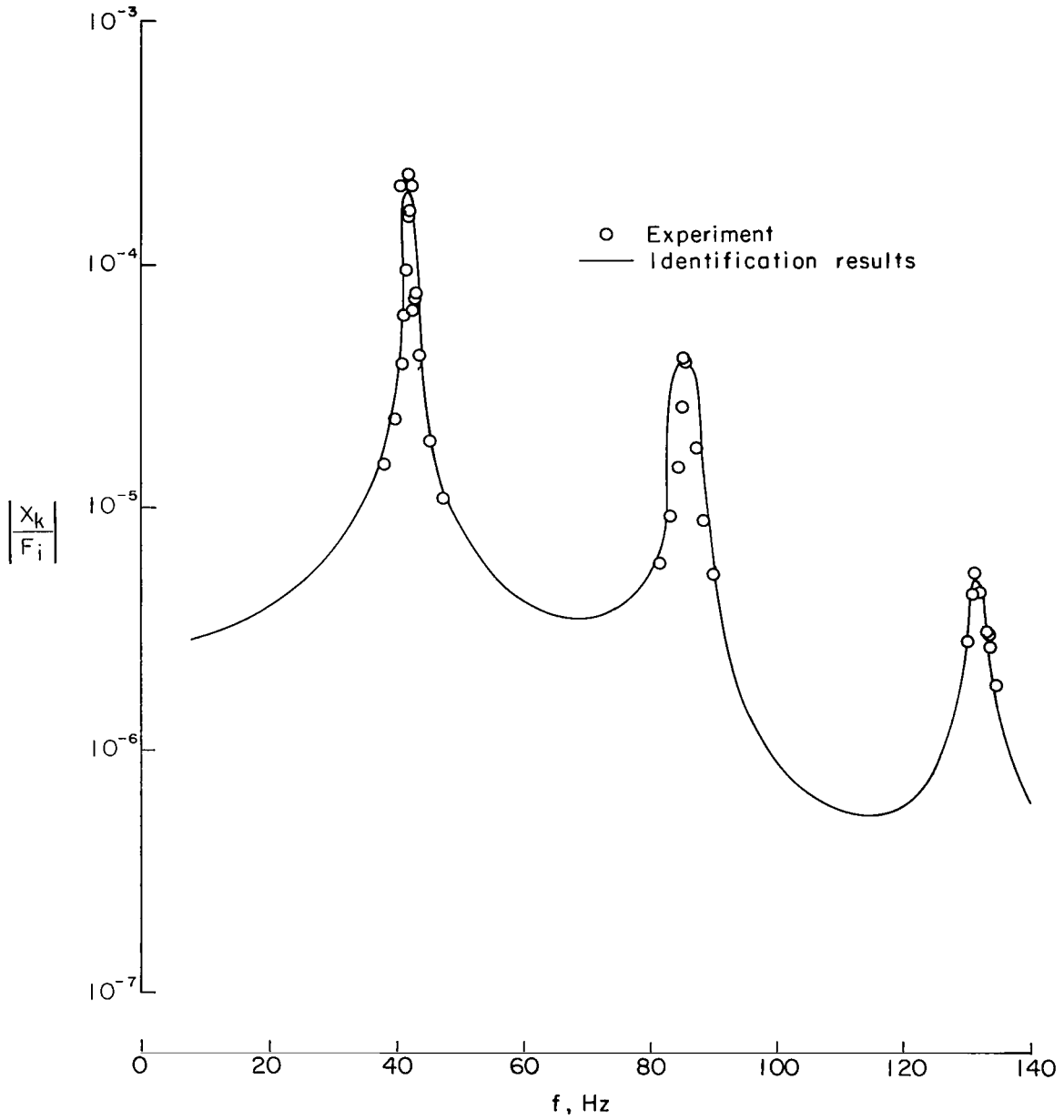

(a) Response at station k = 102.9.

Figure 5.- Comparison of identification results with experimental frequency response for 1/40-scale model forced at station i = 0.

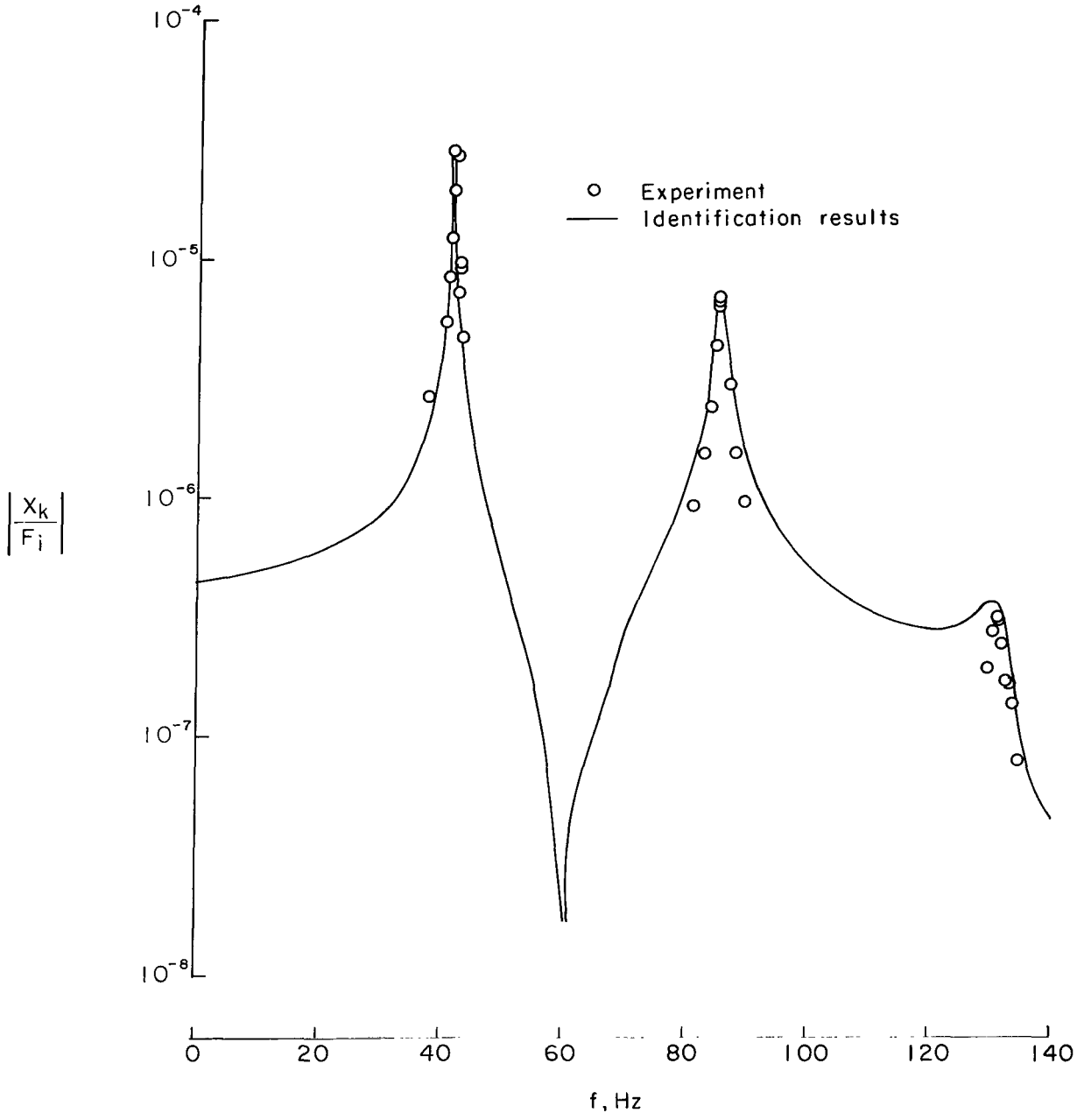

(b) Response at station k = 81.5.

Figure 5.- Continued.

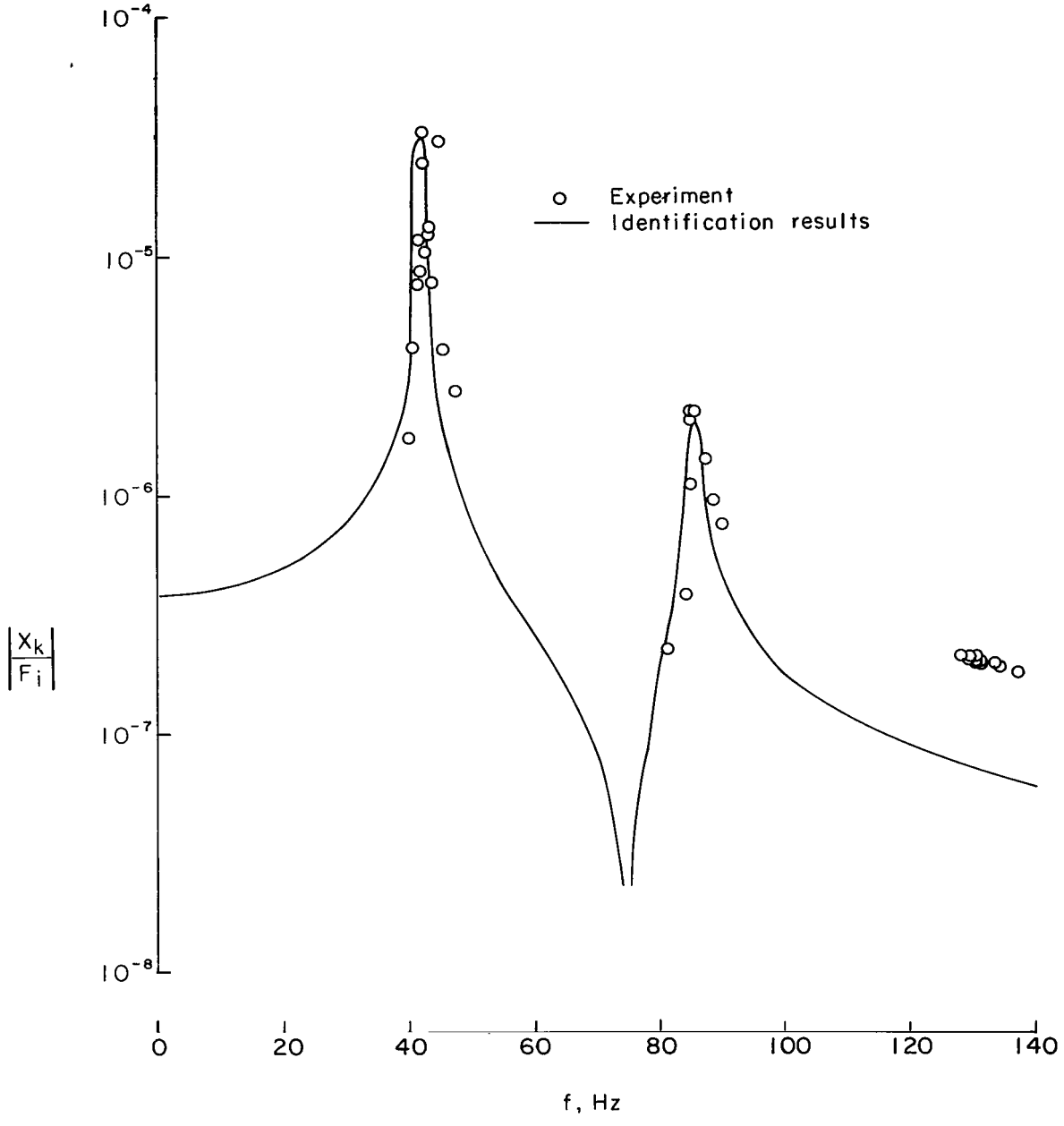

(c) Response at station k = 9.3.

Figure 5.- Continued.

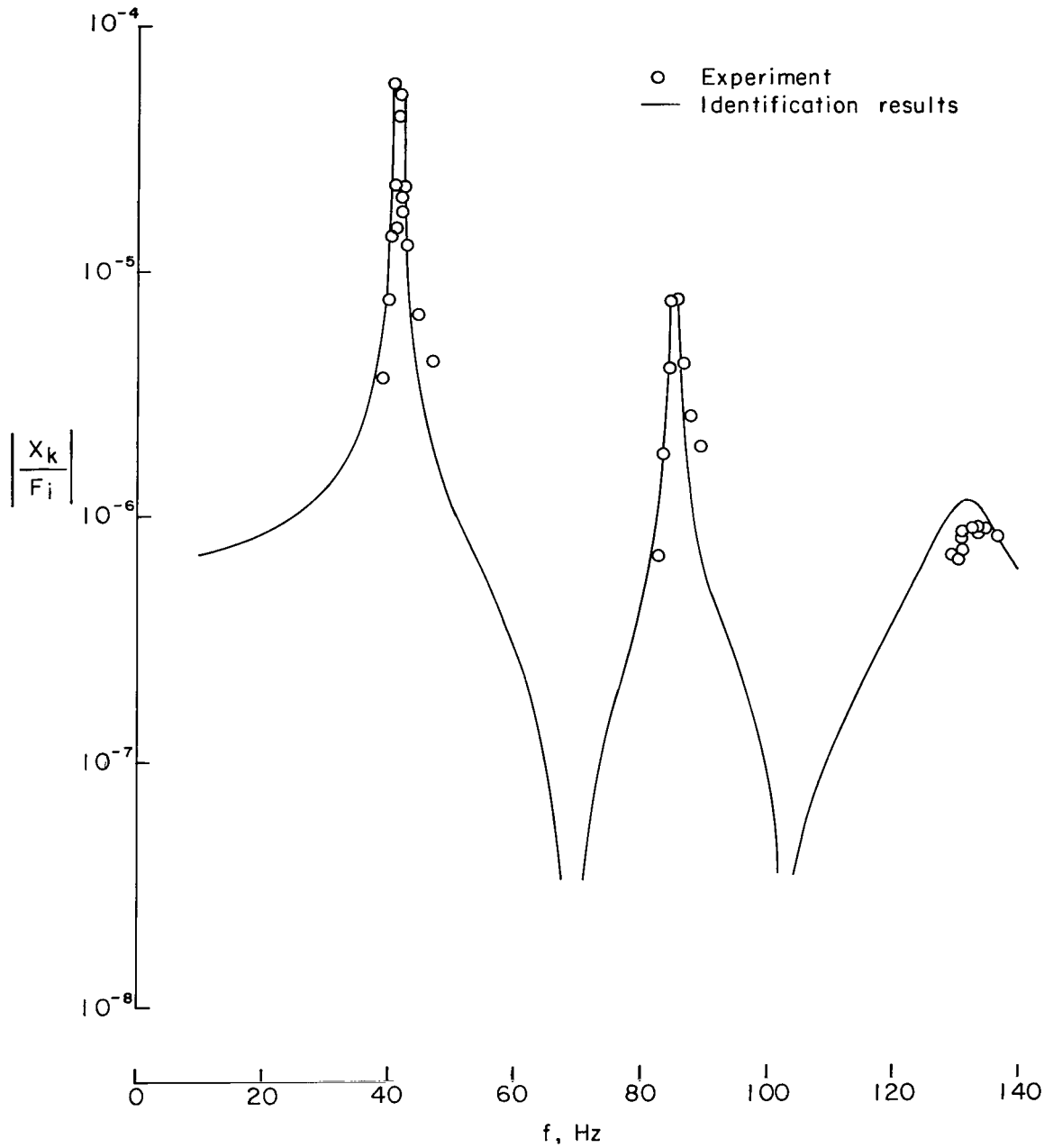

(d) Response at station k = -2.7.

Figure 5.- Concluded.

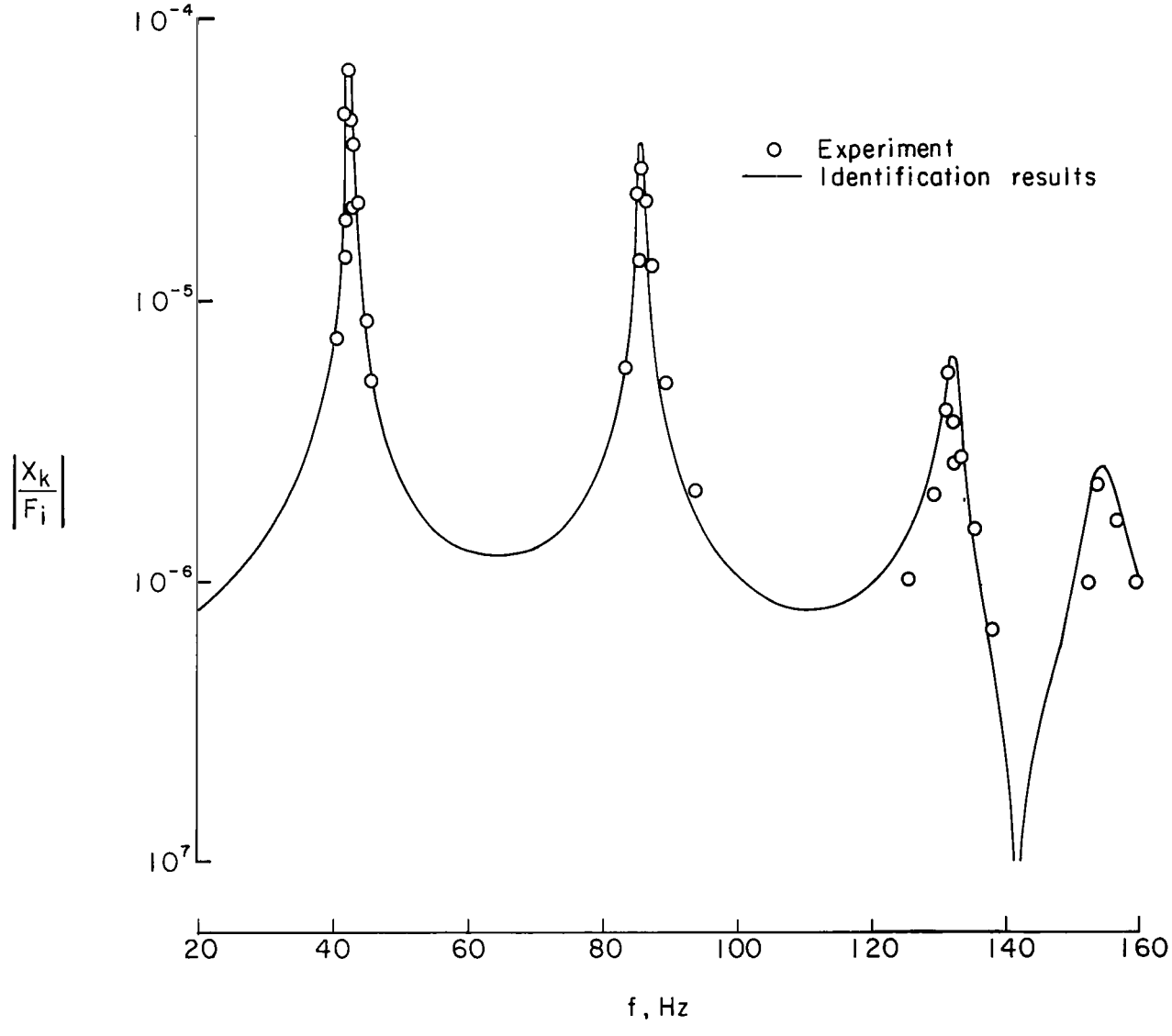

(a) Response at station k = 102.9.

Figure 6.- Comparison of identification results with experimental frequency response for 1/40-scale model forced at station i = 42.

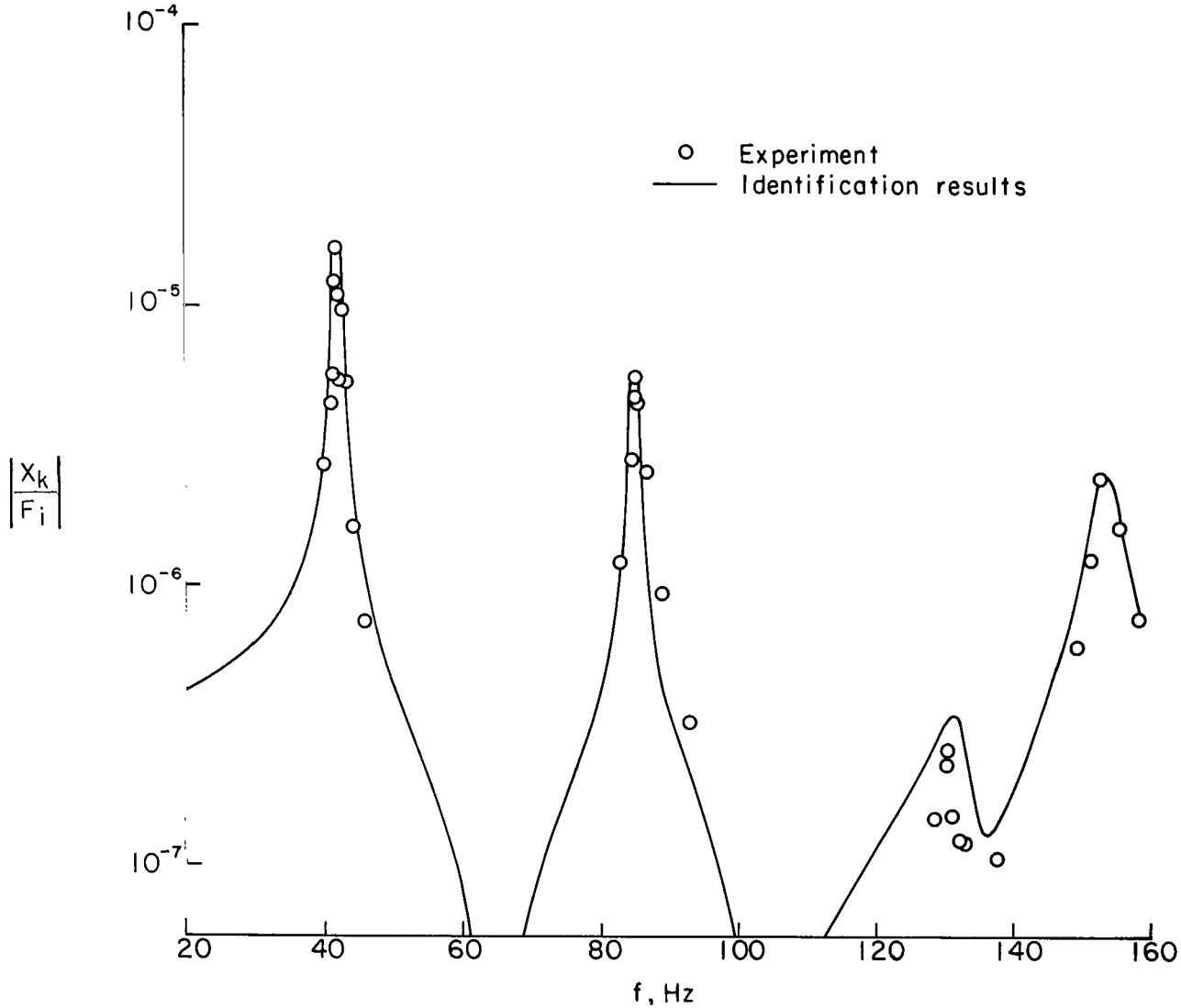

(b) Response at station k = -2.7.

Figure 6.- Concluded.

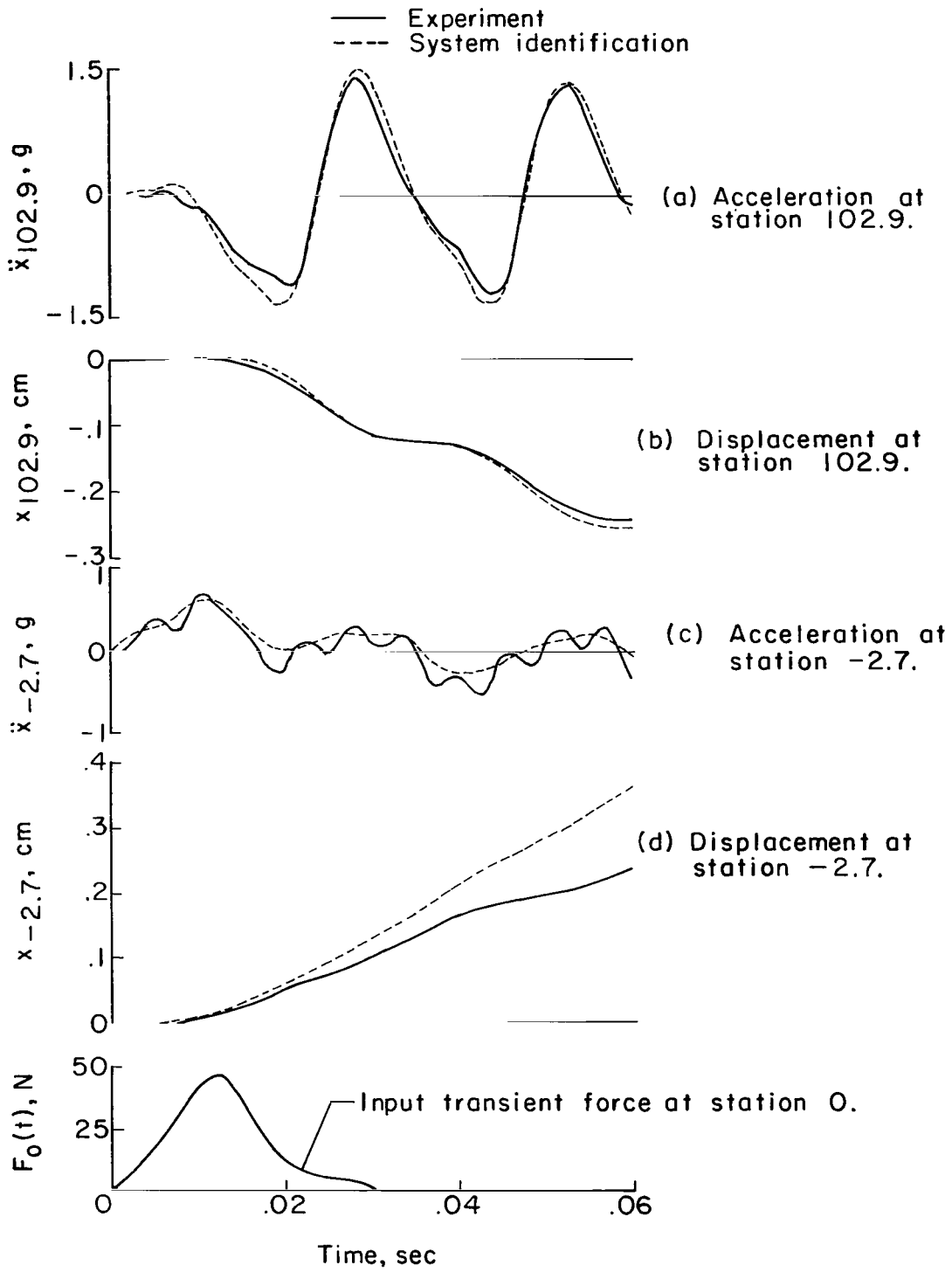

Figure 7.- Comparison of experimental and identification results for transient response of 1/40-scale model forced at station 0.

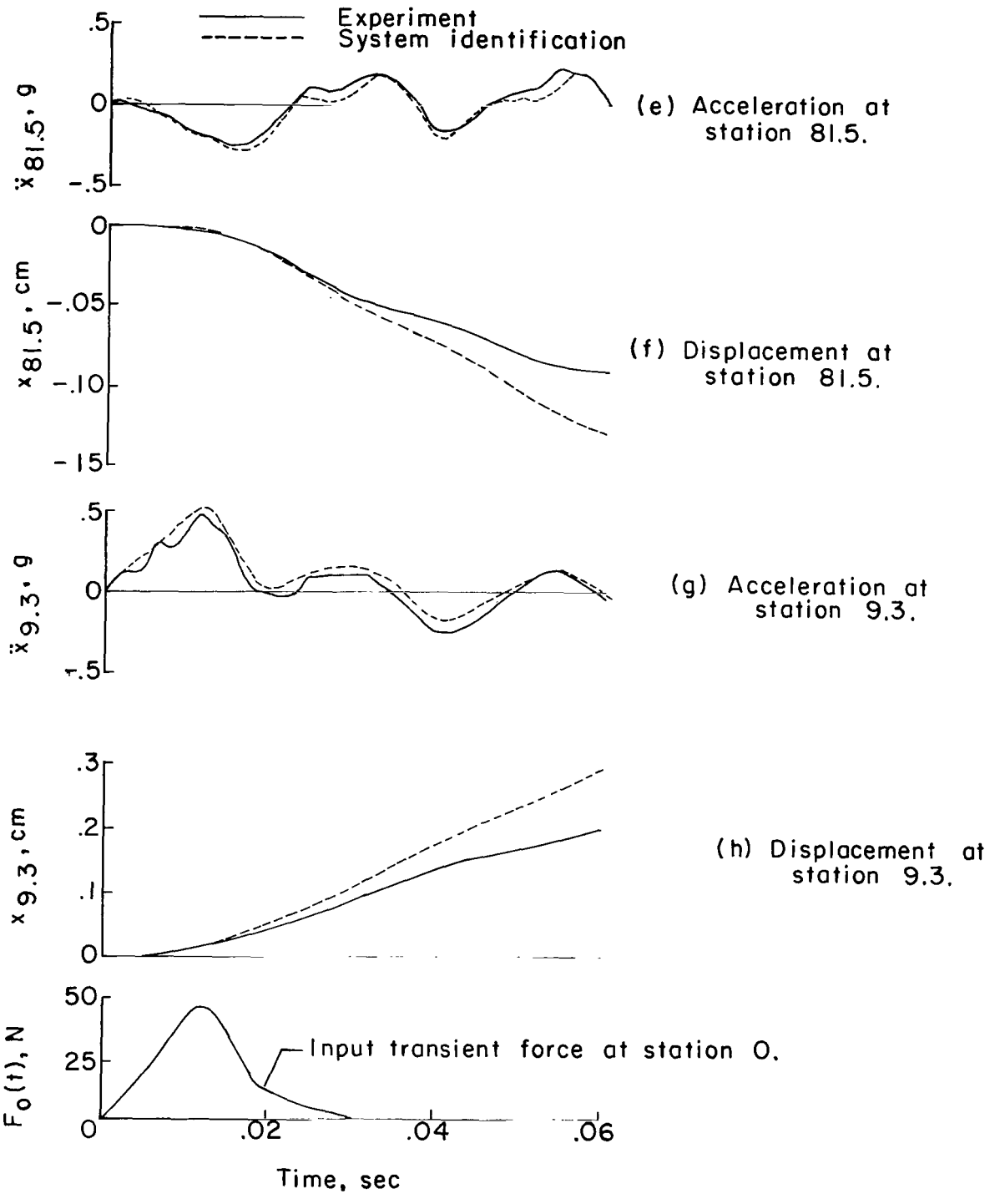

Figure 7.- Concluded.

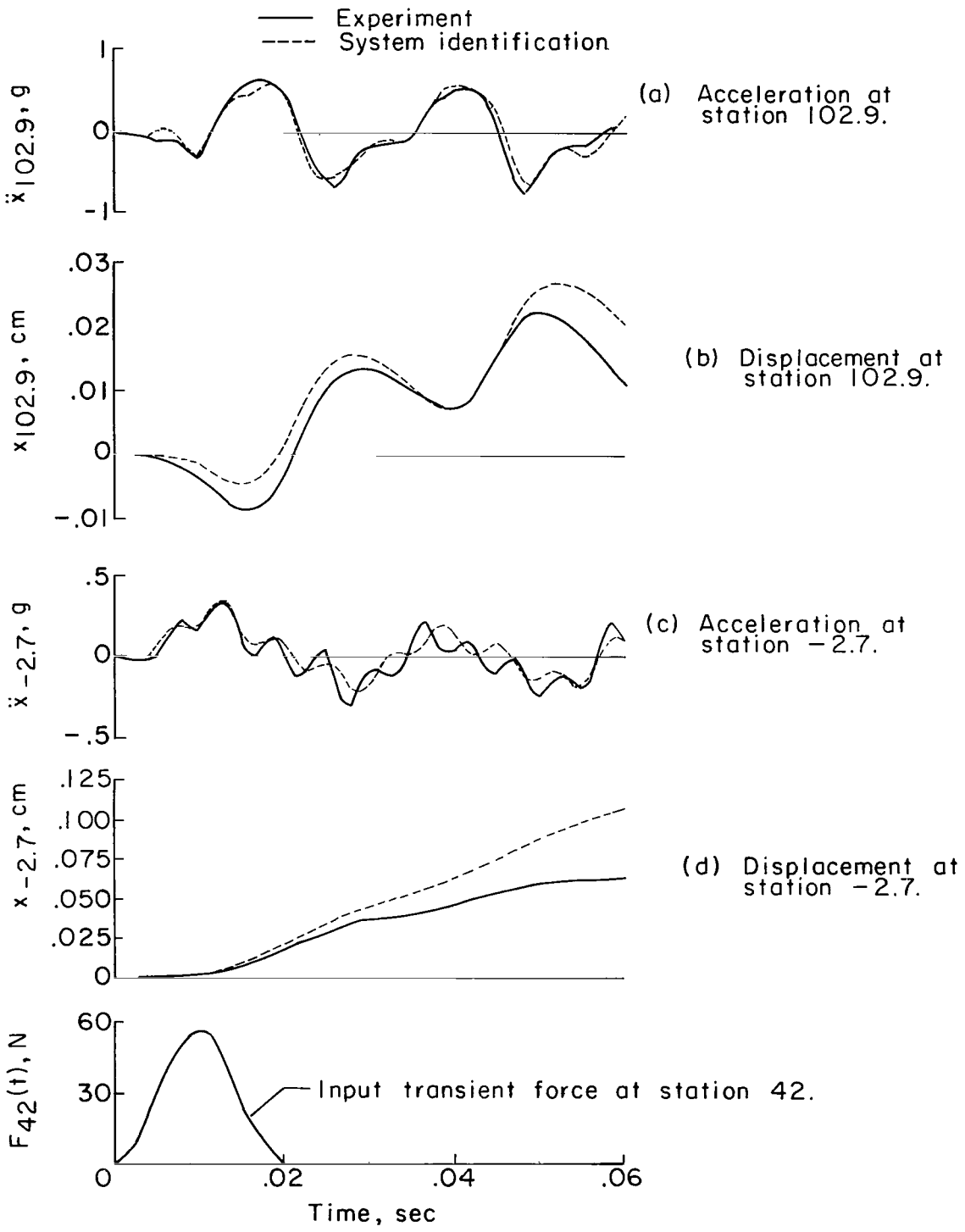

Figure 8.- Comparison of experimental and identification results for transient response of 1/40-scale model forced at station 42.

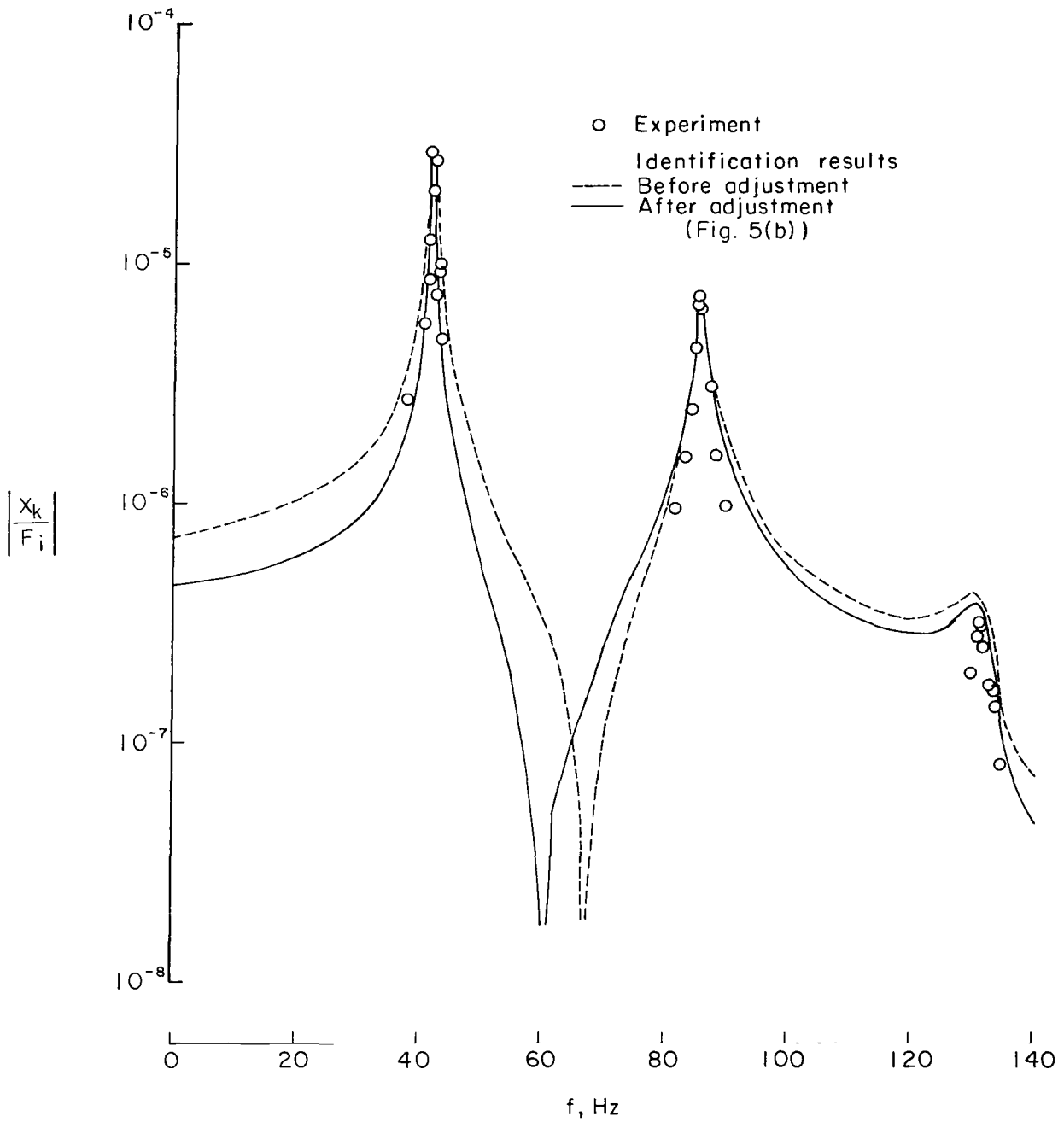

Figure 9.- Amplitude comparison of identification results with experimental results for input force at station i = 0 and point of response at station k = 81.5.

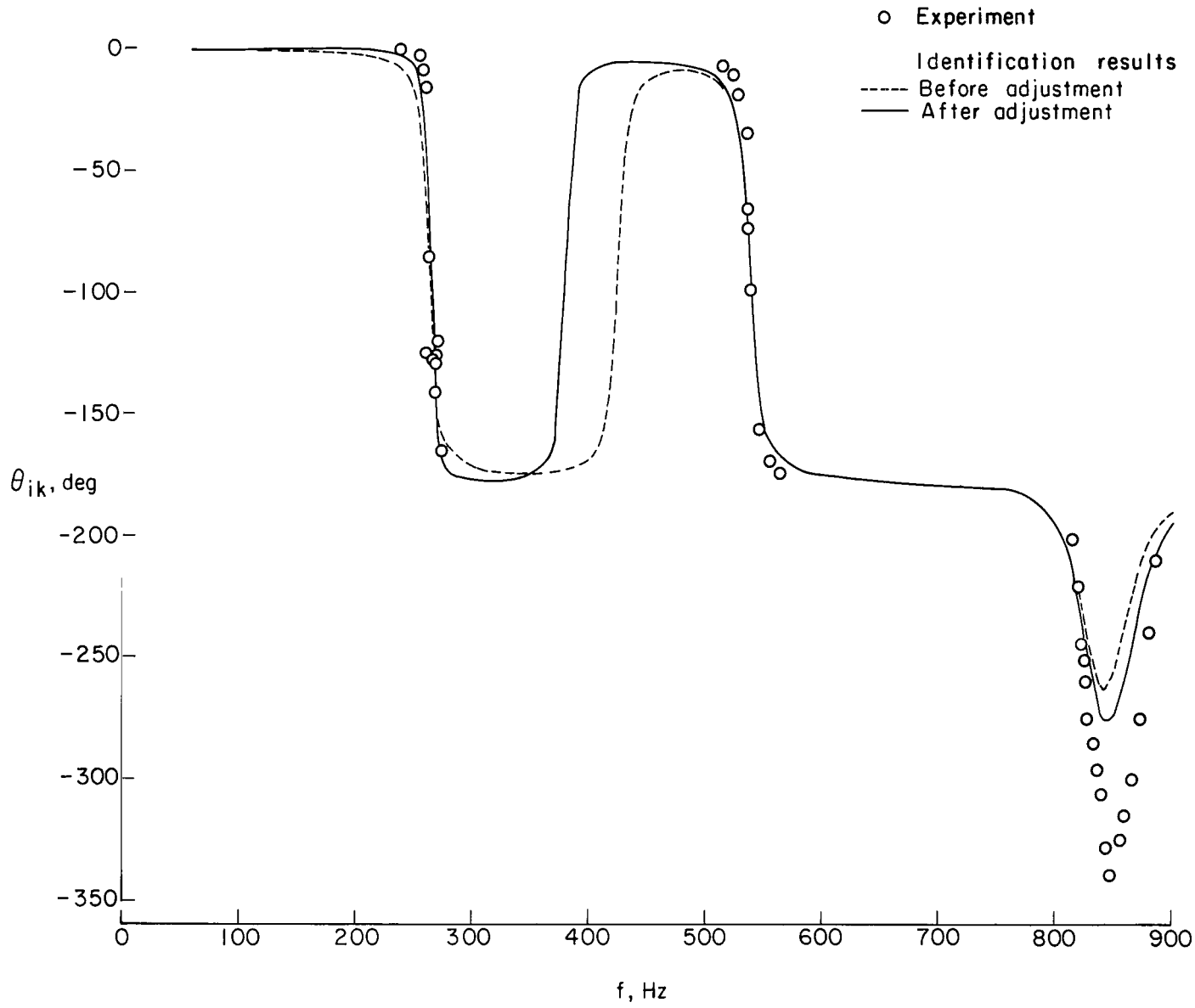

Figure 10.- Phase-angle comparison of identification results with experimental results for input force at station i = 0 and point of response at station k = 81.5.

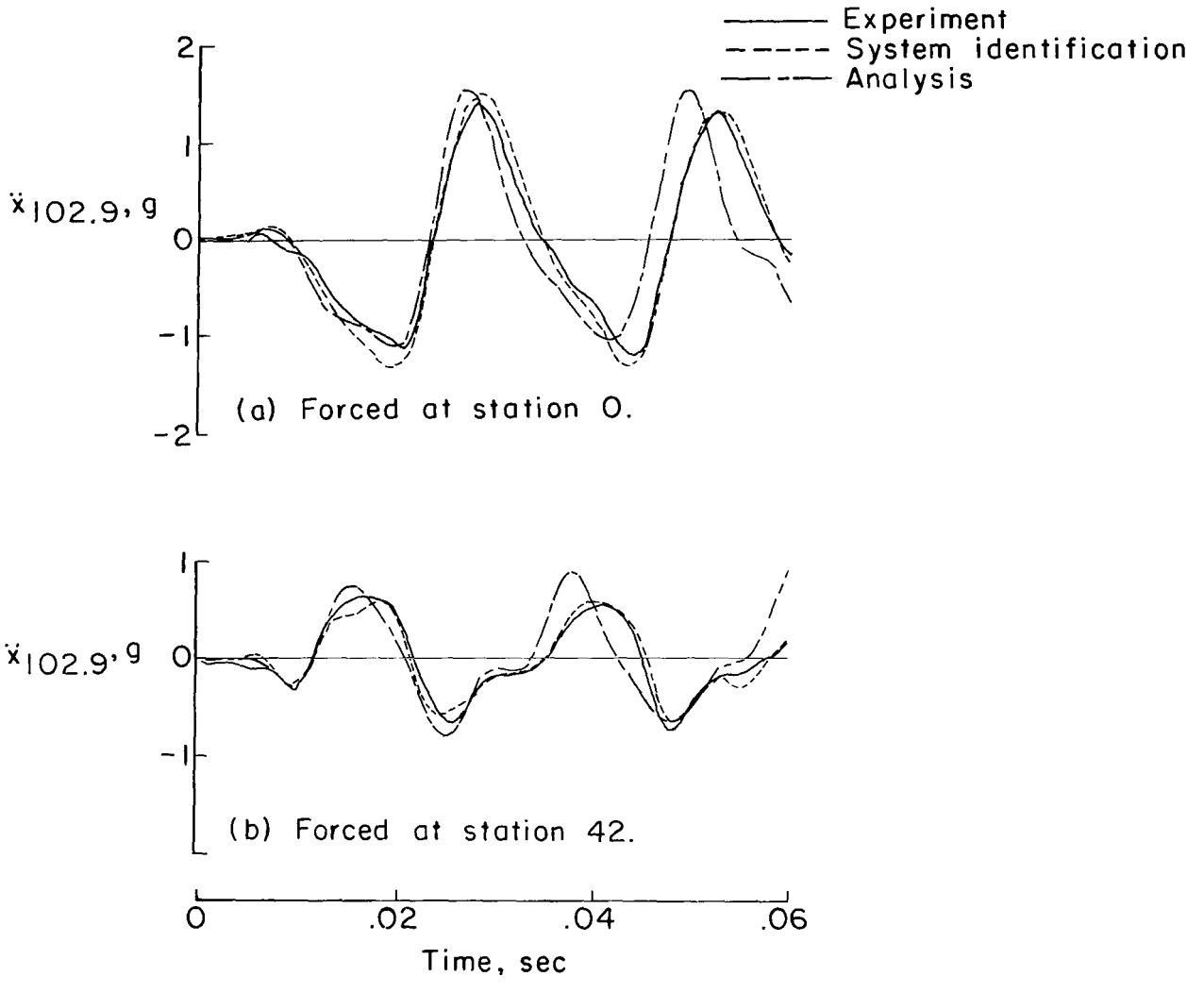

Figure 11.- Comparison of experiment, system identification, and analytically computed transient acceleration response at station 102.9 for the 1/40-scale model.

NASA-Langley, 1969 — 32 L-6325

"The aeronautical and space activities of the United States shall be conducted so as to contribute . . . to the expansion of human knowledge of phenomena in the atmosphere and space. The Administration shall provide for the widest practicable and appropriate dissemination of information concerning its activities and the results thereof."

—NATIONAL AERONAUTICS AND SPACE ACT OF 1958

NASA SCIENTIFIC AND TECHNICAL PUBLICATIONS

TECHNICAL REPORTS: Scientific and technical information considered important, complete, and a lasting contribution to existing knowledge.

TECHNICAL NOTES: Information less broad in scope but nevertheless of importance as a contribution to existing knowledge.

TECHNICAL MEMORANDUMS: Information receiving limited distribution because of preliminary data, security classification, or other reasons.

CONTRACTOR REPORTS: Scientific and technical information generated under a NASA contract or grant and considered an important contribution to existing knowledge.

TECHNICAL TRANSLATIONS: Information published in a foreign language considered to merit NASA distribution in English.

SPECIAL PUBLICATIONS: Information derived from or of value to NASA activities. Publications include conference proceedings, monographs, data compilations, handbooks, sourcebooks, and special bibliographies.

TECHNOLOGY UTILIZATION PUBLICATIONS: Information on technology used by NASA that may be of particular interest in commercial and other non-aerospace applications. Publications include Tech Briefs, Technology Utilization Reports and Notes, and Technology Surveys.

Details on the availability of these publications may be obtained from:

SCIENTIFIC AND TECHNICAL INFORMATION DIVISION

NATIONAL AERONAUTICS AND SPACE ADMINISTRATION

Washington, D.C. 20546